

PROCESS STUDY FOR DEVELOPING ALGORITHMS TO QUANTITATIVELY ESTIMATE HYDROLOGICAL PARAMETERS BASED ON ALOS DATA

PI No 192

Takeo Tadono¹, Nicolas Longepe², and Masanobu Shimada¹

¹ Earth Observation Research Center, Japan Aerospace Exploration Agency, Japan

² CLS, France

1. INTRODUCTION

The objective of this study is to clarify microwave responses for developing algorithms to estimate land hydrological parameters i.e. soil moisture and snow parameters such as snow depth, density, wetness, snow water equivalence (SWE) using PALSAR onboard ALOS. The soil moisture is a key parameter in numerous environmental studies, including hydrology, meteorology, and agriculture. The snow parameters are also important not only hydrology as water resources but also climatology. They play important roles in the interactions between the land surface and the atmosphere, as well as in the partitioning of precipitation into runoff and ground water storage. In spite of such importance, soil moisture is not generally used for weather forecasting because it is difficult to measure on a routine basis over large areas.

This study describes two approaches to consider estimations of surface soil moisture using PALSAR data: 1) applied existing direct algorithm, and 2) applied Electromagnetic (EM) model. The combinations of the estimated soil moisture by passive microwave radiometer are slightly investigated to consider scale-up issues and validation of derived soil moistures, and to use them as *a priori* information to optimize EM model.

2. PREVIOUS STUDIES

Active microwave remote sensors, in particular Synthetic Aperture Radar (SAR) have a potential of observing surface soil moisture with high spatial resolution on a regional scale. In attempting to use SAR image data to estimate soil moisture, several algorithms have been developed [1], [2]. Radar backscatter studies became more rigorous with the availability of polarimetric radar data, and more sophisticated algorithms for estimating soil moisture were presented. Oh et al. developed an empirical model to estimate the root mean square (rms) roughness height and soil moisture from the co-polarized ratio (backscattering ratio of HH and VV polarizations) and the cross-polarized ratio (backscattering ratio of cross and like polarizations) over bare soils of different roughness, and moisture conditions were measured by a truck-mounted scatterometer system [3]. Dubois et al. also developed a model that only requires measurements of HH and VV polarization at frequencies from 1.5 and

11 GHz to retrieve both rms roughness height and soil moisture from bare soil and applied it to the L-band data acquired by both the Airborne SAR (AIRSAR) and Shuttle Imaging Radar-C (SIR-C) over a test site in Oklahoma, US [4]. Hajnsek et al. applied the above two empirical models to L-band data of the airborne Experimental SAR (E-SAR), and compared the performance and accuracy of estimated values [5]. They found that the valid pixels of the E-SAR data decrease to less than 56 % of the total number of pixels. Furthermore, soil moisture was underestimated and roughness was overestimated for both models because the regression fits necessary to estimate the roughness and moisture were dependent on the used data sets. Shi et al. pointed out that neither of the above empirical models considered the surface power spectrum [6]. Furthermore, these empirical models developed from a limited number of observations might have site-specific problems due to nonlinear responses of backscattering to the soil moisture and surface roughness parameters, and an algorithm based on the single-scattering Integral Equation Method (IEM) [7] was developed to estimate soil moisture and surface roughness from dual-polarized SAR measurements and subsequently applied to both AIRSAR and SIR-C data [6]. Consequently, the rms errors were found to be 3.4 % for moisture and 1.9 dB for roughness. However, most of these algorithms have been tested at specific test sites, not under diverse natural surfaces.

3. TEST SITES AND GROUND MEASUREMENTS

Two test sites were used in this study located in Mongolia and Alaska, where spatially homogeneous natural surfaces with basically flat terrain features. Figure 1 shows location of test sites in the Mongolian Plateau, and Figure 2 shows photographs of ground measurement systems: Automatic Weather Stations (AWSs) and Automatic Stations for Soil Hydrology (ASSHs). We were established several test sites in southern part of Ulaanbaatar, Mongolia, and installing and maintaining three AWSs and twelve ASSHs. In addition, intensive experiments have been carried out in summer seasons. Figure 3 shows location of the second test site in the Arctic National Wildlife Refuge (ANWR) which is in northeastern Alaska, US. This extent was covered by tundra vegetation consisting of low shrubs, sedges, and

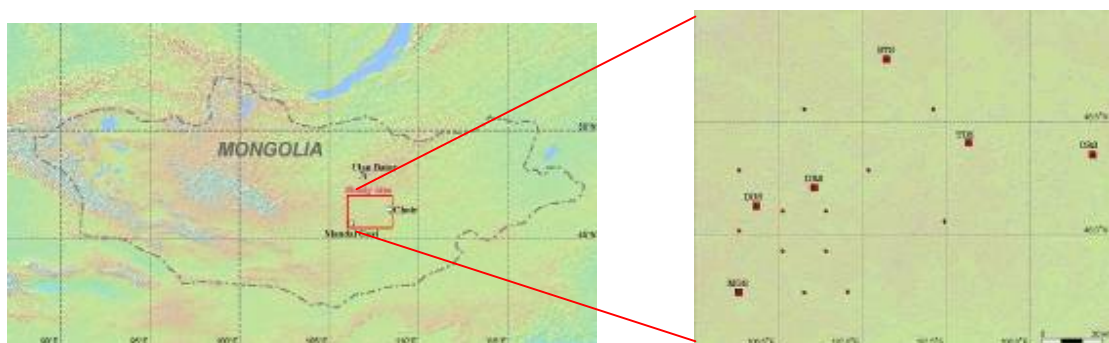


Fig. 1 Location of Mongolian test sites (red squares: AWS sites and red dots: ASSH sites in right)



Fig. 2 Ground-based measuring systems in the Mongolian test sites (left: AWS and right: ASSH)

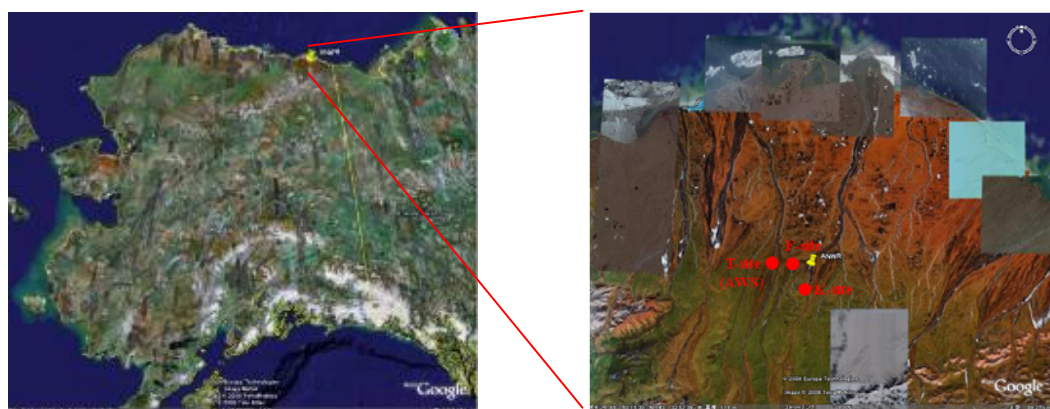


Fig. 3 Location of ANWR test sites in Alaska, US (red dots: field experiment conducted points)



Fig. 4 AWS installed at T site (left), and TDR soil moisture device using the experiment (right) in Alaska, US

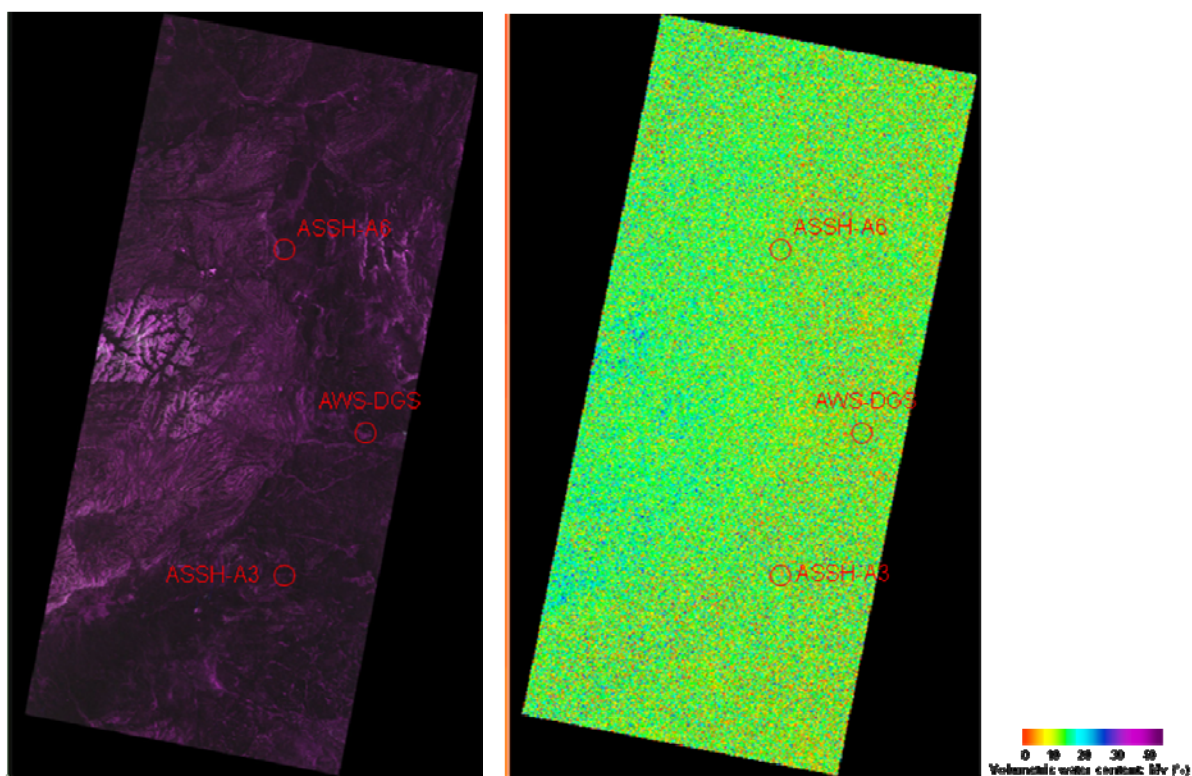


Fig. 5 Color composite of PALSAR (left, R:G:B=VV:HV:HH) and estimated soil moisture map (right) in Mongolian test site on May 25, 2006

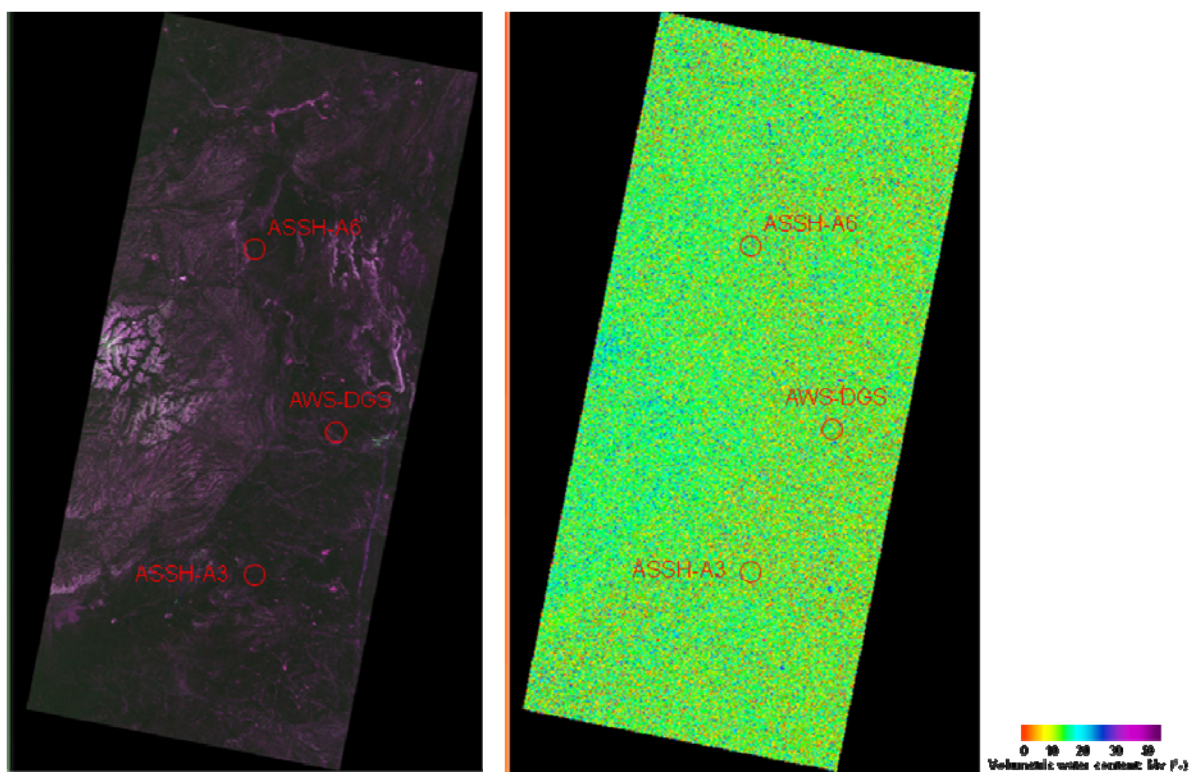


Fig. 6 Color composite of PALSAR (left, R:G:B=VV:HV:HH) and estimated soil moisture map (right) in Mongolian test site on August 25, 2006

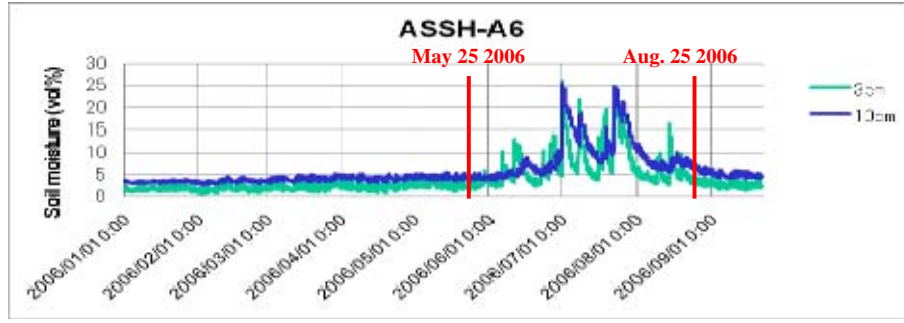


Fig. 7 Time trend of ground based soil moisture by ASSH at A6 site

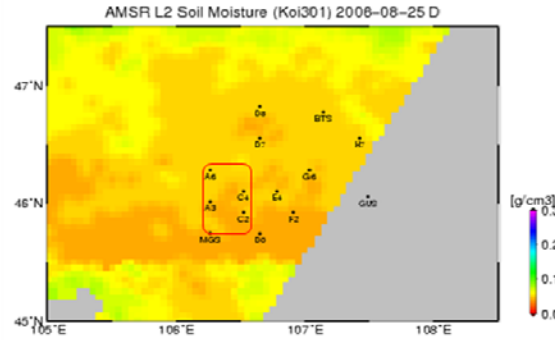


Fig. 8 Soil moisture map derived by AMSR-E on August 25, 2006 (red: coverage of PALSAR images)

mosses. We had been installed an AWS and also carried out a field experiment there from July 25 to August 14, 2008. During the experiment, a simultaneous PALSAR observation was conducted on July 31, 2008. Figure 4 shows AWS and the Time Domain Reflectometry (TDR) soil moisture device using the experiment in Alaska.

4. EXSISTING ALGORITHM BASES APROACH

We firstly applied existing algorithm developed by Shi et al. [6]. The volumetric water content and surface roughness parameters can be separately retrieved using

$$10 \log_{10} \left[\frac{|\alpha_{VV}|^2 + |\alpha_{HH}|^2}{\sigma_{VV}^0 + \sigma_{HH}^0} \right] = a_{VH}(\theta) + b_{VH}(\theta) \times 10 \log_{10} \left[\frac{|\alpha_{VV}| \cdot |\alpha_{HH}|}{\sqrt{\sigma_{VV}^0 \cdot \sigma_{HH}^0}} \right] \quad (1)$$

$$10 \log_{10} \left[\frac{|\alpha_{VV}|^2}{\sigma_{VV}^0} \right] = a_{VV}(\theta) + b_{VV}(\theta) \times 10 \log_{10} \left[\frac{1}{Sr} \right] \quad (2)$$

$$Sr = (k\sigma)^2 \int_0^\infty \rho^n(\xi) J_0(k\xi) \xi d\xi \quad (3)$$

where, $\alpha_{qp}(\theta, \epsilon_r)$: polarization amplitude related to soil moisture, k : wave number, J_0 : Bessel function, and coefficients a , b were defined. The validity range of the algorithm is 2 to 50 vol% of soil moisture, 0.2 to 3.6 cm of rms surface height, 2.5 to 35 cm of surface correlation length, 25 to 70 deg. of incidence angle, and exponential, 1.2 power and 1.4 power correlation functions.

Figure 5 shows color composite images of PALSAR observed by polarimetric mode over the test sites on May

25, 2006 (left) and derived soil moisture map (right) in Mongolian test site. Figure 6 shows same as Figure 5 on August 25, 2006. The red circles indicate locations of test sites, where installed the ground instruments. The retrieval were carried out using original resolution than 8 by 8 pixels corresponding to 100 by 100 meter area averaged soil moisture to reduce effects of speckle noises and uncertainty of inversion processing. The spatial distributions of soil moisture can be identified from Figures 5 and 6, and estimated moisture ranges from 0 to 28 %. The distributions of soil moisture and its characteristics are important in the fields of hydrology and climatology. The estimated soil moisture map on Aug. 25, 2006 is wetter then May 25, 2006 as the result of qualitatively comparison. Figure 7 shows time trend of ground-based soil moisture measured by ASSH at A6 site. This is basically very difficult to compare with estimated soil moisture because it is just point measurement. However, the range of ground measurements is less than 7 %. Therefore, the estimated PALSAR soil moisture is basically over estimation in this case. Figure 8 shows estimated soil moisture using AMSR-E passive microwave radiometer onboard AQUA satellite on Aug. 25, 2006 [8]. The red square indicates location of PALSAR coverage. The averaged soil moisture by AMSR-E is about 5 % over the test site on August 2006. Due to large gaps between both frequencies by PALSAR and AMSR-E, the depths of estimated soil moisture might be different between both estimations in Figures 5, 6 and 8, especially in case of dry soil.

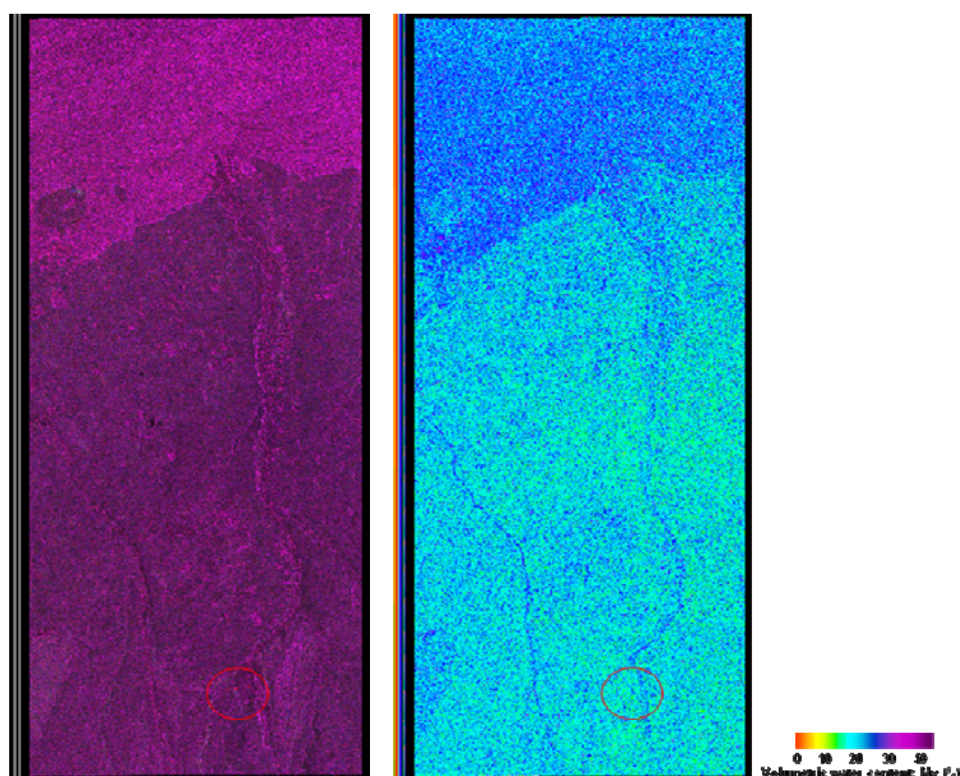


Fig. 9 Color composite of PALSAR (left, R:G:B=VV:HV:HH) and estimated soil moisture map (right) in ANWR, Alaska test site on July 31, 2008

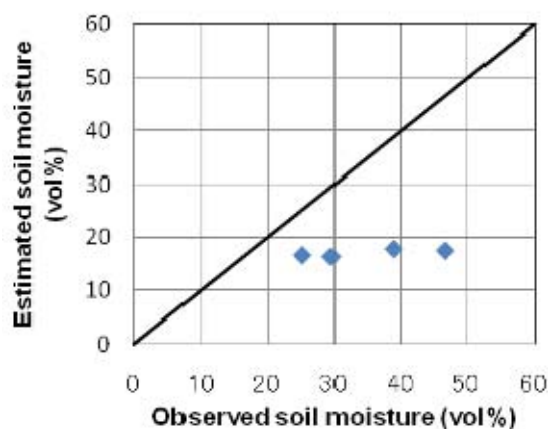


Fig. 10 Comparison of soil moisture between ground measurement and estimated one by PALSAR in ANWR test site on July 31, 2008

The second example used existing algorithm was tested in Alaska test site, US. Figure 9 shows color composite images of PALSAR observed by polarimetric mode over the test sites on July 31, 2008 (left) and derived soil moisture map (right) using eqs. (1) to (3) in Alaska test site. The red circle indicates locations of ANWR test site, where conducted extensive soil moisture observations during the period. They have been observed in four local sites. Each of them had a 100x100 m area per 10 m grids, so total 121 measurement points at each site were made up. The estimated moisture ranges from 3 to 32 % in this region from Figure 9. Figure

10 shows comparison result of soil moisture between ground measurement and estimated PALSAR one at four local sites. This is clearly seen under estimated. We could not say any more quantitatively from these results, and more investigations are necessary with considerations of local incidence angle, roughness and vegetations effects as well as penetration depths depends on moisture conditions. However the algorithm works qualitatively well because Alaska is wetter than Mongolia if compare soil moisture maps between Figures 5 or 6 and 9. That is obviously seeing from both ground measurements and estimated one.

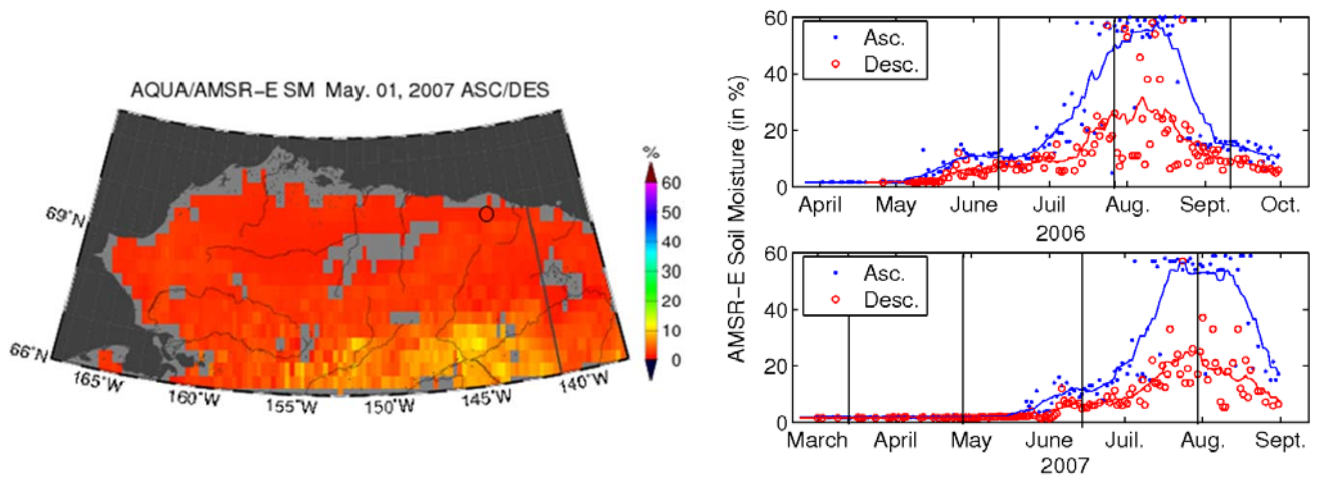


Fig. 11 Example of estimated soil moisture by AMSR-E onboard AQUA (left, black circle indicates location of the ANWR test site), and its time trend in 2006 and 2007 (right, the vertical lines indicate the PALSAR acquisition dates)

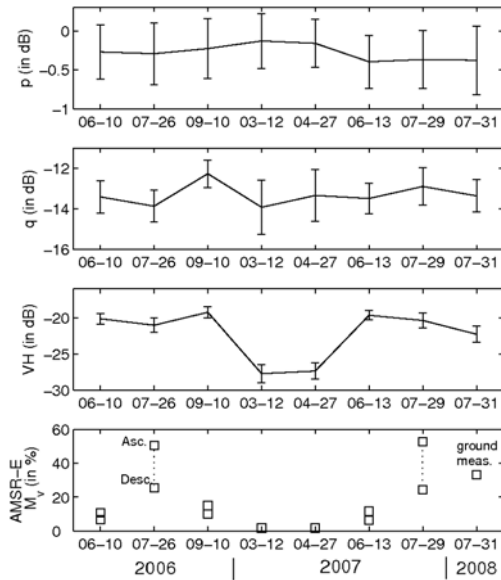


Fig. 12 Analysis of PALSAR data depending on the acquisition date. The error bars correspond to the mean and the standard deviation over an area of 500 by 500 meters

5. EM MODEL APROACH

Next approach is introducing the Electromagnetic (EM) model to concerns not only estimation of soil moisture but also the characterization of permafrost active layer [9]. The ANWR test site in Alaska, US is used in this investigation, and eight fully polarimetric PALSAR data sets were acquired (in June, July, September 2006, March, April, June, July 2007 and July 2008). The effect of vegetated area on the polarimetric signature is still an ongoing topic [10]. Given this uncertainty, the estimation of the residual liquid water in the active layer cannot be assessed through the inversion of a bare soil EM backscattering model. Therefore, the estimated soil moisture by AMSR-E [8] that has high variability as

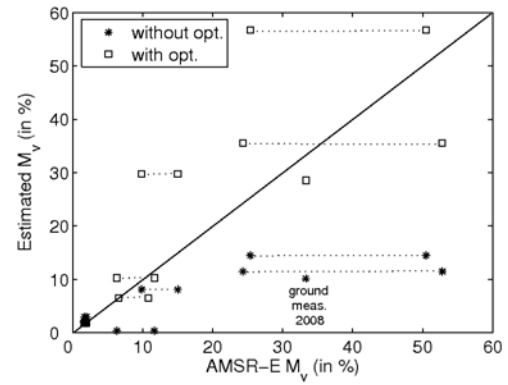


Fig. 13 Comparison between the soil moisture estimated by AMSR-E data and by this methodology

shown in Figure 11, are used as *a priori* qualitative information to optimize the model.

Before the use of any inversion methodology, it appears essential to study the information given by PALSAR data with respect to the *a priori* AMSR-E estimations. Figure 12 presents some polarimetric parameters ($p = \sigma_{HH}^0 / \sigma_{VV}^0$, $q = \sigma_{VH}^0 / \sigma_{VV}^0$ and σ_{VH}^0) depending on the acquisition time. The corresponding soil moistures estimated by AMSR-E in the both orbits of ascending in nighttime and descending in daytime were also given in the bottom of Figure 12. According to AMSR-E estimations, PALSAR data acquired in March and April 2007 correspond to frozen states, whereas those realized in June 2006 and 2007 correspond to thawing states. The polarimetric measurements p and q do not reveal any particular behaviors at these dates. Only the cross-polarized channel HV seems dependent on the liquid water content. Nevertheless, the temporal evolution of the p parameter is theoretically dependent on the soil moisture [11]. If we assume that no significant change of the roughness state occurs over this wild land area, the presence of vegetation may explain this invariant evolution. The values in June

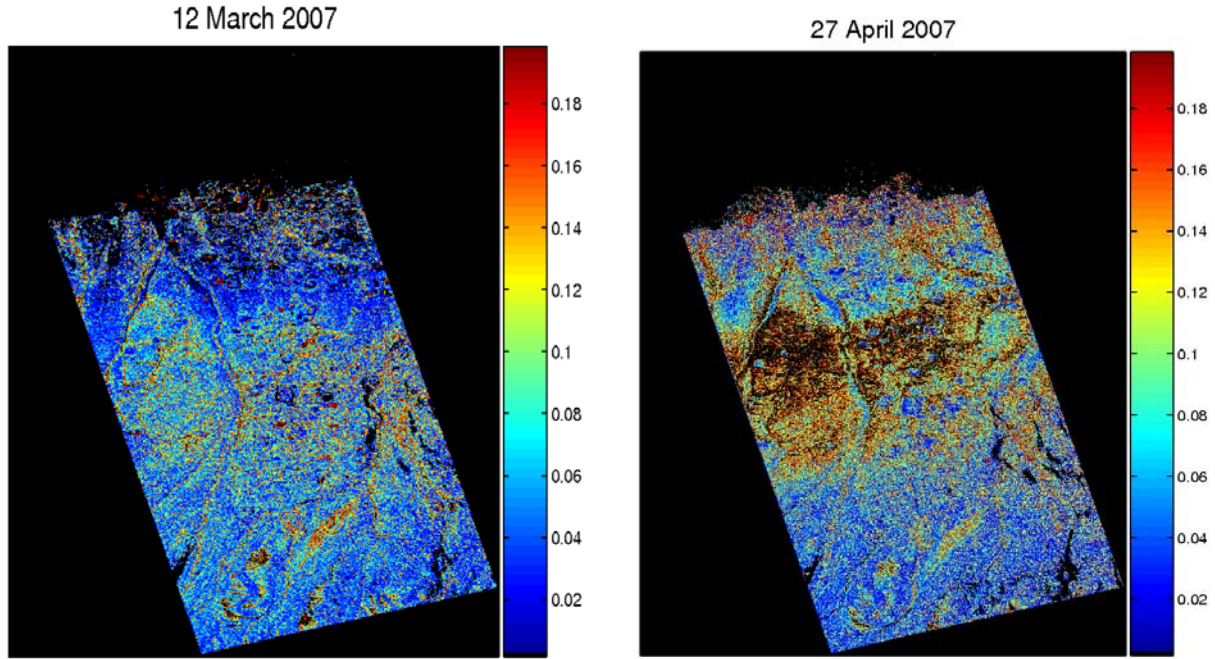


Fig. 14 The estimated soil moisture maps over frozen ground by PALSAR with EM model approach in ANWR, Alaska test site on March 12 (left) and April 27 (right), 2007

2006 and 2007 for σ_{VH}^0 appear to be also invariant with respect to the soil moisture. As confirmed by optical images, the presence of melting snowpack during the thawing period may be an explanation [12]. It is qualitatively shown that the state of arctic tundra and polarimetric PALSAR data establish a confusing relation between the underlying soil properties and polarimetric signature.

Dealing with ground assessments, the necessity for a validated Electromagnetic model is importance. As regards the uncertainties on the vegetation effect, a methodology is proposed in this section. An optimization on the Oh's weights [11] and data is carried out. The estimation of the soil moisture Mv is given as follows [11]

$$Mv = \frac{\omega_1 Mv_1 + \omega_2 Mv_2 + \omega_3 Mv_3}{\omega_1 + \omega_2 + \omega_3} \quad (4)$$

$$\text{with } \begin{aligned} Mv_1 &= f^{-1}(\sigma_{VH}^0, p) \\ Mv_2 &= g^{-1}(q, p) \\ Mv_3 &= h^{-1}(q, \sigma_{VH}^0) \end{aligned} \quad (5)$$

where f , g and h are the Oh's functions [11]. If we assume that the tundra vegetation has a multiplicative and constant effect on the EM model i.e. $\sigma_{HH}^0 = \sigma_{HHpalsar}^0(1 + \omega_4)$, $\sigma_{VV}^0 = \sigma_{VVpalsar}^0(1 + \omega_5)$ and $\sigma_{VH}^0 = \sigma_{VHpalsar}^0(1 + \omega_6)$ the following non-linear problem is solved through a bound-constraint version of the iterative Gauss-Newton algorithm:

$$\arg \min_{\omega_{1-6}} |Mv_{AMSR-E} - Mv|^2 \quad (6)$$

The iteratively Gauss-Newton method is applied using the AMSR-E estimations and PALSAR measurements as inputs of the Oh's models. It should be noted that data acquired in June are not used due to the uncertainty with respect to the snow melt condition. By contrast, data acquired in March and April 2007 are used, assuming a 0.3 density snowpack which modify the f , g and h functions by the three aforementioned effects. As a final result, a new vector ω_{1-6} are estimated. The 3 weights ω_{1-3} are equal to 0.99, 0.54 and 0.50, respectively. For the sake of this case study, this optimization outlines the fact that the equation (4) in [11] is not thoroughly validated within the framework of this inversion. The 3 other weights ω_{4-6} are equal to 0.14, 0.10 and -0.55. These estimations are qualitatively in good agreement with theoretical aspects: vegetation induces an increase of cross-polarized channel (anisotropic effect) and a decrease of co-polarized channels (attenuation mechanism). By applying this weighting, a synthetic bare soil state is retrieved and the estimation of its liquid water content can be finally assessed.

Figure 13 presents the estimated soil moisture with/without this optimization process. It should be noted that a shallow wet snowpack with $\rho=0.3$, $f_{lw}=0.03$ are assumed in June 2006 and 2007, resulting in refractive effects only. PALSAR data have been efficiently constrained by AMSR-E estimations. In a general manner, the Oh's estimates are in a relatively good agreement with AMSR-E data. By tuning PALSAR data and Oh's weights, the effects of vegetation are counterbalanced and

the soil moisture can be efficiently estimated. Figure 14 shows estimated PALSAR soil moisture maps over frozen soil based on this analysis on March and April 2007. Note that the color bars are different with Figure 9's one, however the spatial distribution of Figure 14 looks reasonable.

6. SUMMARY AND CONCLUSIONS

This study tried to estimate surface soil moisture using PALSAR especially using polarimetry data. Ideally, PALSAR has longer wavelength as L-band thus relatively less sensitive for surface roughness and vegetations. We applied two methods over natural terrains in Mongolia and Alaska, where are located in seasonal permafrost regions. Basically, the Mongolia test site is significantly dry condition, meanwhile the Alaska site is wet condition. In the case of applying the existing algorithm developed by Shi et al. based on IEM model simulations without tuning, the overestimated soil moisture was obtained in Mongolia, and the underestimated one was in Alaska as quantitatively evaluation results. Even so, it works qualitatively well if compare estimated soil moisture between both sites. These results suggested that we should be carefully considering effects of roughness, vegetation, local incidence angle, terrain, as well as penetration depth of microwave.

In the second case based on EM model analysis, the estimated soil moistures by passive microwave radiometer were used to optimize the model as *a priori* qualitative information. This could be enhanced the range of estimated PALSAR soil moisture, and derived spatial and temporal changes of soil moisture distributions. Such optimization is highly recommended as to "remove" irrelevant effects as mentioned above.

7. REFERENCES

[1] J. R. Wang et al., "The SIR-B observations of microwave dependence on soil moisture, surface roughness and vegetation covers", IEEE Trans. Geoscience Remote Sensing, vol.GE-24, pp.510-516, 1986.
 [2] T. Tadono et al., "Development of an algorithm for soil moisture mapping based on single-parameter SAR images in permafrost regions including the effect of surface roughness", Journal of Hydroscience and Hydraulic Engineering, vol.18, no.1, 2000.

[3] Y. Oh et al., "An empirical model and inversion technique for radar scattering from bare soil surface", IEEE Trans. Geoscience Remote Sensing, vol.30, pp.370-378, 1992.
 [4] P. C. Dubois et al., "Measuring soil moisture with imaging radar", IEEE Trans. Geoscience Remote Sensing, vol.33, pp.915-926, 1995.
 [5] I. Hajnsek et al., "Determination of hydrological parameters using Airborne-Radar data (DLR E-SAR)", Proceedings IGARSS '99, IEEE, pp.1108-1110, 1999.
 [6] J. Shi et al., "Estimation of bare soil moisture and surface roughness parameter using L-band SAR image data", IEEE Trans. Geoscience Remote Sensing, vol.35, no.5, pp.1254-1266, 1997.
 [7] A. K. Fung, "Microwave scattering and emission models and their applications", Artech house, 1994.
 [8] T. Koike et al., "Development of an Advanced Microwave Scanning Radiometer (AMSR-E) algorithm for soil moisture and vegetation water content," Annual journal of Hydraulic Engineering, JSCE, 2004.
 [9] N. Longepe et al., "Case studies of frozen ground monitoring using PALSAR/ALOS data," Proceedings IGARSS 2009, IEEE, 2009.
 [10] I. Hajnsek et al., "Potential of estimating soil moisture under vegetation cover by means of PolSAR," IEEE Trans. Geoscience Remote Sensing, vol. 47, no. 2, pp. 442-454, 2009.
 [11] Y. Oh, "Quantitative retrieval of soil moisture content and surface roughness from multipolarized radar observations of bare soil surfaces," IEEE Trans. Geoscience Remote Sensing, vol.42, no.3, pp.596-601, 2004.
 [12] N. Longepe et al., "Capabilities of full polarimetric PALSAR/ALOS for snow extent mapping," Proceedings IGARSS 2008, IEEE, 2008.

ACKNOWLEDGEMENT

The authors wish to thank Prof. Ichirow Kaihotsu for maintaining ground instruments in Mongolia, and Dr. Manabu Watanabe, Dr. Kim Yongwon, Prof. Keiji Kushida, and Prof. Mamoru Ishikawa for collecting the ground truth data in ANWR, Alaska in 2007 acquired under the collaboration between the International Arctic Research Center (IARC) and JAXA.